LOOP ANTENNAS

The *IEEE Standard Definitions of Terms for Antennas* (see Ref. 1) defines the loop antenna as "an antenna whose configuration is that of a loop," further noting that "if the current in the loop, or in the multiple parallel turns of the loop, is essentially uniform and the loop circumference is small compared with the wavelength, the radiation pattern approximates that of a magnetic dipole." That definition and the further note imply the two basic realms of loop antennas: electrically small and electrically large structures.

There are more than 200 million loop antennas currently used by subscribers of personal communications devices, primarily pagers [see Ref. (2)]. More than a million a month are currently being manufactured. Furthermore, loops have appeared as transmitting arrays, such as the massive multielement loop array at shortwave station, call sign HCJB, in Quito, Ecuador, and as fractional wavelength-size tunable high-frequency transmitting antennas. The loop is indeed an important and pervasive communications antenna.

The following analysis of loop antennas reveals that the loop, when small compared with a wavelength, exhibits a radiation resistance proportional to the square of the enclosed area. Extremely low values of radiation resistance are encountered for such loops, and extreme care must be taken to effect efficient antenna designs. Furthermore, when the small loop is implemented as a transmitting resonant circuit, surprisingly high voltages can exist across the resonating capacitor even for modest applied transmitter power levels. The wave impedance in the immediate vicinity of the loop is low but at further distances (up to 2 wavelengths) exceeds the intrinsic free-space impedance before approaching that value.

A loop analysis is summarized, which applies to loops of arbitrary circular diameter and of arbitrary wire thickness. The analysis leads to some detail regarding the current density in the cross section of the wire. Loops of shapes other than circular are less easily analyzed, and are best handled by numerical methods such as moment method described in Ref. 3.

Loops are the antennas of choice in pager receivers and appear as both ferrite-loaded loops and as single-turn rectangular shaped structures within the radio housing. Body-worn loops benefit from a field enhancement due to the resonant behavior of the human body with respect to vertically polarized waves. In the high-frequency bands, the loop is used as a series resonant circuit fed by a secondary loop. The structure can be tuned over a very large frequency band while maintaining a relatively-constant-feed point impedance. Large loop arrays of one-wavelength-perimeter square loops have been successfully implemented as high-gain transmitting structures at high-power shortwave stations.

ANALYSIS OF LOOP ANTENNAS

Loop antennas, particularly circular loops, were among the first radiating structures analyzed, beginning as early as 1897 with Pocklington's analysis of a thin wire loop excited by a plane wave (4). Later, Hallén (5) and Storer (6) studied driven loops. All these authors used a Fourier expansion of the loop current, and the latter two authors discovered numerical difficulties with the approach. The difficulties could be avoided, as pointed out by Wu (7), by integrating the Green's function over the toroidal surface of the wire. The present author coauthored an improved theory (8,9) that specifically takes into account the finite dimension of the loop wire and extends the validity of the solution to thicker wires than previously considered. Additionally, the work revealed some detail of the loop current around the loop cross section. Arbitrarily shaped loops, such as triangular loops and square loops, as well as loop arrays can be conveniently analyzed using numerical methods, such as by the moment method (3).

The Infinitesimal Loop Antenna

The infinitesimal single turn current loop consists of a circulating current I enclosing an infinitesimal surface area S, and is solved by analogy to the infinitesimal dipole. The fields of an elementary loop element of radius b can be written in terms of the loop enclosed area, $S = \pi b^2$, and a constant excitation current I (when I is rms, then the fields are also rms quantities). The fields are "near" in the sense that the distance parameter r is far smaller than the wavelength but far larger than the loop dimension $2b$. Hence, this is *not* the *close* near-field region. The term kIS is often called the loop moment and is analogous to the similar term Ih associated with the dipole moment. The infinitesimally small loop is pictured in Fig. 1(a) next to its elementary dipole analog [Fig. 1(b)].

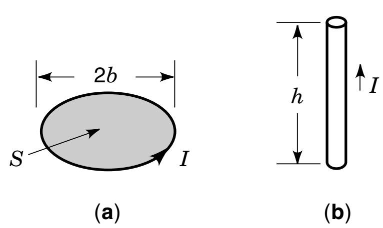

Figure 1. Small-antenna geometry showing (a) the parameters of the infinitesimal loop moment, and (b) its elementary dipole dual. [Source: Siwiak (2).]

The dipole uniform current I flowing over an elemental length h is the dual of a "magnetic current" $M_zS = Ih$ and the surface area is $S = h/k$. The fields due to the infinitesimal loop are then found from the vector and scalar potentials.

Vector and Scalar Potentials. The wave equation, in the form of the inhomogeneous Helmholtz equation, is used here with most of the underlying vector arithmetic omitted; see Refs. 10 to 12 for more details. For a magnetic current element source, the electric displacement $\boldsymbol{D}$ is always solenoidal (the field lines do not originate or terminate on sources), that is, in the absence of source charges the divergence is zero,

$$\nabla \cdot \boldsymbol{D} = 0 \tag{1}$$

and the electric displacement field can be represented by the curl of an arbitrary vector $\boldsymbol{F}$,

$$\boldsymbol{D} = \epsilon_0 \boldsymbol{E} = \nabla \times \boldsymbol{F} \tag{2}$$

where $\boldsymbol{F}$ is the vector potential and obeys the vector identity $\nabla \cdot \nabla \times \mathbf{F} = 0$. Using Ampere's law in the absence of electric sources

$$\nabla \times \boldsymbol{H} = j\omega\epsilon_0 \boldsymbol{E} \tag{3}$$

and with the vector identity $\nabla \times (-\nabla\Phi) = 0$, where Φ represents an arbitrary scalar function of position, it follows that

$$\boldsymbol{H} = -\nabla\Phi - j\omega\boldsymbol{F} \tag{4}$$

and for a homogeneous medium, after some manipulation we get

$$\nabla^2\boldsymbol{F} + k^2\boldsymbol{F} = -\epsilon_0\boldsymbol{M} + \nabla(\nabla \cdot \boldsymbol{F} + j\omega\mu_0\epsilon_0\Phi) \tag{5}$$

where k is the wave number and $k^2 = \omega^2\mu_0\epsilon_0$. Although Eq. (2) defines the curl of $\boldsymbol{F}$, the divergence of $\boldsymbol{F}$ can be independently defined and the *Lorentz condition* is chosen:

$$j\omega\mu_0\epsilon_0\Phi = -\nabla \cdot \boldsymbol{F} \tag{6}$$

We define ∇^2 as the Laplacian operator

$$\nabla^2 = \frac{\partial^2}{\partial x^2} + \frac{\partial^2}{\partial y^2} + \frac{\partial^2}{\partial z^2} \tag{7}$$

Substituting the simplification of Eq. (6) into Eq. (5) leads to the inhomogeneous Helmholtz equation

$$\nabla^2\boldsymbol{F} + k^2\boldsymbol{F} = -\epsilon_0\boldsymbol{M} \tag{8}$$

Similarly, by using Eqs. (6) and (4) it is seen that

$$\nabla^2\Phi + k^2\Phi = 0 \tag{9}$$

Using Eq. (4) and the Lorentz condition of Eq. (6) we can find the electric field solely in terms of the vector potential $\boldsymbol{F}$. The utility of that definition becomes apparent when we consider a magnetic current source aligned along a single vector direction, for example, $\boldsymbol{M} = \boldsymbol{z}M_z$ for which the vector potential is $\boldsymbol{F} = \boldsymbol{z}F_z$, where $\boldsymbol{z}$ is the unit vector aligned with the z axis, and Eq. (8) becomes a scalar equation.

Radiation from a Magnetic Current Element. The solution to the wave equation, Eq. (8), presented here, with the details suppressed, is a spherical wave. The results are used to derive the radiation properties of the infinitesimal current loop as the dual of the infinitesimal current element. The infinitesimal magnetic current element $\boldsymbol{M} = \boldsymbol{z}M_z$ located at the origin satisfies a one-dimensional, hence scalar form of Eq. (8). At points excluding the origin where the infinitesimal current element is located, Eq. (8) is source-free and is written as a function of radial distance r,

$$\nabla^2 F_z(r) + k^2 F_z(r) = \frac{1}{r^2}\frac{\partial}{\partial r}\left(r^2 \frac{\partial F_z(r)}{\partial r}\right) + k^2 F_z(r) = 0 \qquad (10)$$

which can be reduced to

$$\frac{d^2 F_z(r)}{dr^2} + \frac{2}{r}\frac{dF_z(r)}{dr} + k^2 F_z(r) = 0 \qquad (11)$$

Since F_z is a function of only the radial coordinate, the partial derivative in Eq. (10) was replaced with the ordinary derivative. Equation (11) has a solution

$$F_z = C_1 \frac{e^{-jkr}}{r} \qquad (12)$$

There is a second solution in which the exponent of the phasor quantity is positive; however, we are interested here in outward traveling waves so we discard that solution. In the static case the phasor quantity is unity. The constant C_1 is related to the strength of the source current and is found by integrating Eq. (8) over the volume including the source, giving

$$C_1 = \frac{\epsilon_0}{4\pi} kIS \qquad (13)$$

and the solution for the vector potential is in the $\boldsymbol{z}$ unit vector direction,

$$\boldsymbol{F} = \frac{\epsilon_0}{4\pi} kIS \frac{e^{-jkr}}{r}\boldsymbol{z} \qquad (14)$$

which is an outward propagating spherical wave with increasing phase delay (increasingly negative phase) and with amplitude decreasing as the inverse of distance. We may now solve for the magnetic fields of an infinitesimal current element by inserting Eq. (14) into Eq. (4) with Eq. (6) and then for the electric field by using Eq. (2). The fields, after sufficient manipulation, and for $r \gg kS$ (see Ref. 10), are

$$H_{\mathrm{r}} = \frac{kIS}{2\pi} e^{-jkr} k^2 \left(\frac{j}{(kr)^2} + \frac{1}{(kr)^3}\right)\cos(\theta) \qquad (15)$$

$$H_\theta = \frac{kIS}{4\pi} e^{-jkr} k^2 \left(-\frac{1}{kr} + \frac{j}{(kr)^2} + \frac{1}{(kr)^3}\right)\sin(\theta) \qquad (16)$$

$$E_\phi = \eta_0 \frac{kIS}{4\pi} e^{-jkr} k^2 \left(\frac{1}{kr} - \frac{j}{(kr)^2}\right)\sin(\theta) \qquad (17)$$

where $\eta_0 = c\mu_0 = 376.730313$ is the intrinsic free-space impedance, c is the velocity of propagation in free space (see Ref. 13 for definitions of constants), and I is the loop current.

Equations (15) and (16) for the *magnetic* fields H_{r} and H_θ of the infinitesimal loop have exactly the same form as the *electric* fields E_{r} and E_θ for the infinitesimal dipole, while Eq. (17) for the *electric* field of the loop E_ϕ has exactly the same form as the *magnetic* field H_ϕ of the dipole when the term kIS of the loop expressions is replaced with Ih for the infinitesimal ideal (uniform current element) dipole. In the case for which the loop moment kIS is superimposed on, and equals the dipole moment Ih, the fields in all space will be circularly polarized.

Equations (15) to (17) describe a particularly complex field behavior for what is a very idealized selection of sources: a simple linear magnetic current M representing a current loop I encompassing an infinitesimal surface $S = \pi b^2$. Equations (15) to (17) are valid only in the region sufficiently far ($r \gg kS$) from the region of the magnetic current source M.

The Wave Impedance of Loop Radiation. The wave impedance can be defined as the ratio of the total electric field divided by the total magnetic field. We can study the wave impedance of the loop fields by using Eqs. (15) to (17) for the infinitesimal loop fields, along with their dual quantities for the ideal electric dipole. Figure 2 shows the loop field wave impedance as a function of distance kr from the loop along the direction of maximum far-field radiation. The wave impedance for the elementary dipole is shown for comparison. At distances near $kr = 1$ the wave impedance of loop radiation exceeds $\eta_0 = 376.73\ \Omega$, the intrinsic free-space impedance, while that of the infinitesimal loop is below 376.73 Ω. In this region, the electric fields of the loop dominate.

The Radiation Regions of Loops. Inspection of Eqs. (15) to (17) for the loop reveal a very complex field structure. There are components of the fields that vary as the inverse third power of distance r, inverse square of r, and the inverse of r. In the near-field or induction region of the idealized infinitesimal loop, that is, for $kr \ll 1$ (however, $r \gg kS$ for the loop and $r \gg h$ for the dipole), the magnetic fields vary as the inverse third power of distance.

The region in which kr is nearly unity is part of the radiating near field of the Fresnel zone. The inner boundary of that

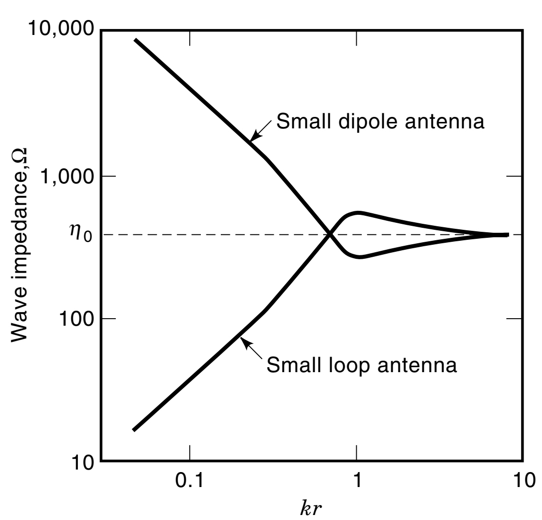

Figure 2. Small loop antenna and dipole antenna wave impedances compared. [Source: Siwiak (2).]

zone is taken by Jordan and Balmain (12) to be $r^2 > 0.38D^3/\lambda$, and the outer boundary is $r > 2D^2/\lambda$, where D is the largest dimension of the antenna, here equal to $2b$. The outer boundary criterion is based on a maximum phase error of $\pi/8$. There is a significant radial component of the field in the Fresnel zone.

The far field or Fraunhofer zone is the region of the field for which the angular radiation pattern is essentially independent of distance. That region is usually defined as extending from $r < 2D^2/\lambda$ to infinity, and the field amplitudes there are essentially proportional to the inverse of distance from the source. The far-zone behavior is identified with the basic free-space propagation law.

The Induction Zone of Loops. We can study the *induction zone* in comparison to the *far field* by considering induction zone coupling, which was investigated by Hazeltine (14), and which was applied to low-frequency radio receiver designs of his time. Today the problem might be applied to the design of a miniature radio module in which inductors must be oriented for minimum coupling. The problem Hazeltine solved was one of finding the geometric orientation for which two loops in parallel planes have minimum coupling in the induction zone of their near fields and serves to illustrate that the "near-field" behavior differs fundamentally and significantly from "far-field" behavior. To study the problem we invoke the principle of reciprocity (see Ref. 10), which states

$$\int_V (\boldsymbol{E}_{\mathrm{b}} \cdot \boldsymbol{J}_{\mathrm{a}} - \boldsymbol{H}_{\mathrm{b}} \cdot \boldsymbol{M}_{\mathrm{a}})\, dV = \int_V (\boldsymbol{E}_{\mathrm{a}} \cdot \boldsymbol{J}_{\mathrm{b}} - \boldsymbol{H}_{\mathrm{a}} \cdot \boldsymbol{M}_{\mathrm{b}})\, dV \qquad (18)$$

That is, the reaction on antenna (a) of sources (b) equals the reaction on antenna (b) of sources (a). For two loops with loop moments parallel to the z axis we want to find the angle θ for which the coupling between the loops vanishes, that is, both sides of Eq. (18) are zero. The reference geometry is shown in Fig. 3. In the case of the loop, there are no electric sources in Eq. (18), so $\boldsymbol{J}_{\mathrm{a}} = \boldsymbol{J}_{\mathrm{b}} = \mathbf{0}$, and both $\boldsymbol{M}_{\mathrm{a}}$ and $\boldsymbol{M}_{\mathrm{b}}$ are aligned with $\boldsymbol{z}$, the unit vector parallel to the z axis. Retaining only the inductive field components and clearing common constants in Eqs. (15) and (17) are placed into (18). We require that $(H_r\boldsymbol{r} + H_\theta\boldsymbol{\theta})\boldsymbol{z} = 0$. Since $\boldsymbol{r}\cdot\boldsymbol{z} = -\sin(\theta)$ and $\boldsymbol{\theta}\cdot\boldsymbol{z} = \cos(\theta)$, we are left with $2\cos^2(\theta) - \sin^2(\theta) = 0$, for which $\theta = 54.736°$. When oriented as shown in Fig. 3, two loops parallel to the x–y plane whose centers are displaced by an angle of 54.736° with respect to the z axis will not couple in their near fields. To be sure, the angle determined above is "exactly" correct for infinitesimally small loops; however, that angle will be nominally the same for larger loops. Hazeltine (14) used this principle, placing the axes of the inductors in a common plane each at an angle of 54.7° with respect to the normal form the radio chassis, to minimize the coupling between the inductors.

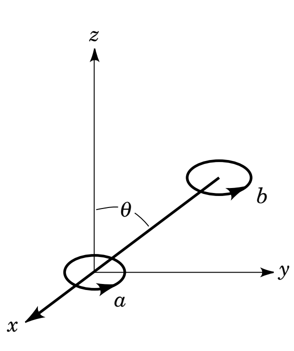

Figure 3. Two small loops in parallel planes and with $\theta = 54.736°$ will not couple in their near fields. [Source: Siwiak (2).]

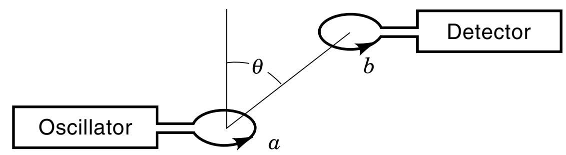

Figure 4. A metal detector employs two loops initially oriented to minimize coupling in their near fields.

The same principle can be exploited in the design of a metal detector, as depicted in Fig. 4. The loop a is driven with an audio frequency oscillator. Loop b, in a parallel plane and displaced so that nominally $\theta = 54.7°$, is connected to a detector that might comprise an audio amplifier that feeds a set of headphones. Any conductive object near loop a will disrupt the balance of the system and result in an increased coupling between the two loops, thus indicating the presence of a conducting object near a.

The Intermediate- and Far-Field Zones of Loops. The loop-coupling problem provides us with a way to investigate the intermediate- and far-field coupling by applying Eq. (18) with Eqs. (15) and (16) for various loop separations kr. In the far-field region only the H_θ term of the magnetic field survives, and by inspection of Eq. (16), the minimum coupling occurs for $\theta = 0°$ or 180°. Figure 5 compares the coupling (normalized to their peak values) for loops in parallel planes whose fields are given by Eqs. (15) to (17). Figure 5 shows the coupling as a function of angle θ for an intermediate region ($kr = 2$) and for the far-field case ($kr = 1000$) in comparison with the induction zone case ($kr = 0.001$). The patterns are fundamentally and significantly different. The coupling null at $\theta = 54.7°$ is clearly evident for the induction zone case $kr = 0.001$ and for which the $(1/kr)^3$ terms dominate. Equally evident is the far-field coupling null for parallel loops on a common axis when the $1/kr$ terms dominate. The intermediate-zone cou-

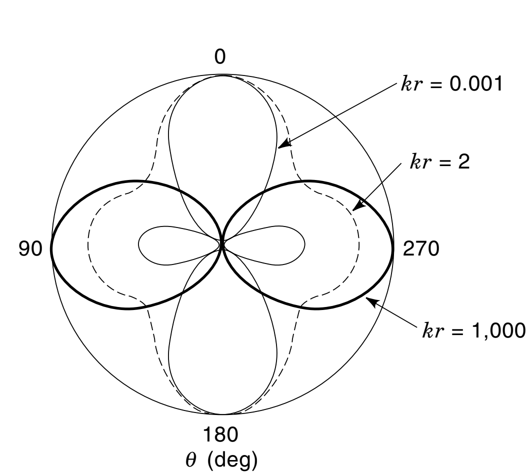

Figure 5. Normalized induction zone, intermediate zone, and far zone coupling between loops in parallel planes. [Source: Siwiak (2).]

pling shows a transitional behavior in which all the terms in kr are comparable.

The Directivity and Impedance of Small Loops. The *directive gain* of the electrically small loop can be found from the far-field radially directed Poynting vector in ratio to the average Poynting vector over the radian sphere:

$$D(\theta,\phi) = \frac{|(\boldsymbol{E}\times\boldsymbol{H}^{*})\cdot\boldsymbol{r}|}{\dfrac{1}{4\pi}\displaystyle\int_0^{2\pi}\int_0^{\pi}|(\boldsymbol{E}\times\boldsymbol{H}^{*})\cdot\boldsymbol{r}|\sin(\theta)\,d\theta\,d\phi} \tag{19}$$

Only the θ component of $\boldsymbol{H}$ and the ϕ component of $\boldsymbol{E}$ survive into the far field. If we use Eq. (16) for H_θ and Eq. (17) for E_ϕ and retain only the $1/kr$ terms, Eq. (19) yields $D = 1.5 \sin^2(\theta)$ by noting that the functional form of the product of E and H is simply $\sin^2(\theta)$ and by carrying out the simple integration in the denominator of Eq. (19).

Taking into account the directive gain, the far-field power density P_d in the peak of the pattern is

$$P_{\mathrm{d}} = \frac{1.5I^2R_{\mathrm{r}}}{4\pi r^2} = H_\theta^2\eta_0 = \left(\frac{kS}{4\pi}\frac{k}{r}I\right)^2\eta_0 \tag{20}$$

for radiated power I^2R_r, hence, we can solve for the radiation resistance:

$$R_{\mathrm{r}} = \frac{(k^2S)^2}{6\pi}\eta_0 = \eta_0\frac{\pi}{6}(kb)^4 \tag{21}$$

for the infinitesimal loop of loop radius b.

When fed by a gap, there is a dipole moment that adds terms not only to the impedance of the loop but also to the close near fields. For the geometry shown in Fig. 6, and using the analysis of King and Harrison (15), the electrically small loop, having a diameter $2b$ and wire diameter $2a$, exhibits a feed point impedance given by

$$\begin{aligned} Z_{\mathrm{loop}} &= \eta_0\frac{\pi}{6}(kb)^4[1+8(kb)^2]\left(1-\frac{a^2}{b^2}\right)\cdots \\ &\quad + j\eta_0 kb\left[\ln\left(\frac{8b}{a}\right)-2+\frac{2}{3}(kb)^2\right][1+2(kb)^2] \end{aligned} \tag{22}$$

including dipole mode terms valid for $kb \ll 0.1$. The leading term of Eq. (22) is the same as derived in Eq. (21) for the infinitesimal loop. Expression (22) adds the detail of terms considering the dipole moment of the gap fed loop as well as refinements for loop wire radius a. The small loop antenna is characterized by a radiation resistance that is proportional to the fourth power of the loop radius b. The reactance is inductive, hence, is proportional to the loop radius. It follows that the Q, the quality factor defined in (2), is inversely proportional to the third power of the loop radius, a result that is consistent with the fundamental limit behavior for small antennas.

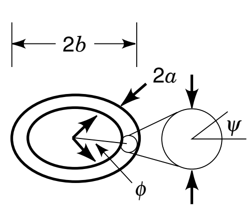

Figure 6. Parameters of the thick-wire loop. [Source: Siwiak (2).]

If we use Eq. (22) and ignore the dipole mode terms and second-order terms in a/b, the unloaded Q of the loop antenna is

$$Q_{\mathrm{loop}} = \frac{\dfrac{6}{\pi}\left[\ln\left(\dfrac{8b}{a}\right)-2\right]}{(kb)^3} \tag{23}$$

which for $b/a = 6$ becomes

$$Q_{\mathrm{loop}} = \frac{3.6}{(kb)^3} \tag{24}$$

which has the proper limiting behavior for small loop radius. The Q of the small loop given by Eq. (23) is indeed larger than the minimum possible $Q_{\min} = (kb)^{-3}$ predicted by Siwiak (2) for a structure of its size. It must be emphasized that the actual Q of such an antenna will be smaller than given by Eq. (24) due to unavoidable dissipative losses not represented in Eqs. (22) to (24). We can approach the minimum Q but never go smaller, except by introducing dissipative losses.

The Gap-Fed Loop

The analysis of arbitrarily thick wire loops follows the method in Ref. 8, shown in simplified form in Ref. 9 and summarized here. The toroid geometry of the loop is expressed in cylindrical coordinates ρ, ϕ, and z with the toroid located symmetrically in the $z = 0$ plane. The relevant geometry is shown in Fig. 6.

Loop Surface Current Density. The current density on the surface of the toroidal surface of the loop is given by

$$J_\phi = \sum_{n=-\infty}^{\infty}\sum_{p=-\infty}^{\infty} B_{n,p}e^{jn\phi}F_p \tag{25}$$

where the functions F_p are symmetrical about the z axis and are simple functions of $\cos(n\psi)$, where ψ is in the cross section of the wire as shown in Fig. 6 and is related to the cylindrical coordinate by $z = a\sin(\psi)$. These functions are orthonormalized over the conductor surface using the Gram–Schmidt method described in Ref. 16, yielding

$$F_0 = \frac{1}{2\pi\sqrt{ab}} \tag{26}$$

and

$$F_1 = F_0\sqrt{\frac{2}{1-(a/2b)^2}}\left(\cos(\psi)-\frac{a}{2b}\right) \tag{27}$$

The higher-order functions are lengthy but simple functions of $\sin(p\psi)$ and $\cos(p\psi)$.

Scalar and Vector Potentials. The electric field is obtained from the vector and scalar potentials

$$\boldsymbol{E} = -\nabla\Phi - j\omega\boldsymbol{A} \tag{28}$$

The boundary conditions require that E_ϕ, E_ψ, and E_ρ are zero on the surface of the loop everywhere except at the feed gap $|\phi| \leq \epsilon$. Because this analysis will be limited to wire diameters significantly smaller than a wavelength, the boundary conditions on E_ψ and E_ρ will not be enforced. In the gap $E_\phi = V_0/2\epsilon\rho$, where V_0 is the gap excitation voltage.

The components of the vector potential are simply

$$A_\phi = \frac{1}{4\pi}\int_S\int J_\phi \cos(\phi - \phi')\, dS \tag{29}$$

and

$$A_\rho = \frac{1}{4\pi}\int_S\int J_\phi \sin(\phi - \phi')\, dS \tag{30}$$

and the vector potential is

$$\Phi = \frac{j\eta_0}{4\pi k}\int_S\int \frac{1}{\rho}\frac{\partial J_\phi}{\partial \phi} G\, dS \tag{31}$$

where the value of $dS = [b + a\sin(\psi)]a\, d\psi$. The Green's function G is expressed in terms of cylindrical waves to match the rotational symmetry of the loop,

$$G = \frac{1}{2j}\sum_{m=-\infty}^{\infty} e^{-jm(\phi-\phi')}\int_{-\infty}^{\infty} J_m(\rho_1 - v)H_m^{(2)}(\rho_2 - v)e^{-j\zeta(z-z')}\, d\zeta \tag{32}$$

where

$$v = \sqrt{k^2 + \zeta^2}$$
$$\rho_1 = \rho - a\cos(\psi)$$
$$\rho_2 = \rho + a\cos(\psi)$$

and where $J_m(\nu\rho)$ and $H_m^{(2)}(\nu\rho)$ are the Bessel and Hankel functions.

Matching the Boundary Conditions. Expression (32) is now inserted into Eqs. (29) to (31) and the electric field is then found from Eq. (28) and the boundary condition is enforced. For constant ρ on the wire

$$\int_{-\pi}^{\pi} E_\phi e^{jp\phi}\, d\phi = -\frac{V_0}{\rho}\frac{\sin(p\epsilon)}{p\epsilon} \tag{33}$$

This condition is enforced on the wire as many times as there are harmonics in ψ. Truncating the index p as described in Ref. 9 to a small finite number P, we force $E_\phi = 0$ except in the feeding gap along the lines of constant ρ on the surface of the toroid. If we truncate to P, the number of harmonics F_p in ψ, and to M the number of harmonics in ϕ, we find the radiation current by solving M systems of P by P algebraic equations in $B_{m,p}$. In Ref. 9, $P = 2$ and M in the several hundreds was found to be a reasonable computational task that led to useful solutions.

Loop Fields and Impedance. With the harmonic amplitudes $B_{m,p}$ known, the current density is found from Eq.(1). The electric field is found next from Eq. (2) and the magnetic field is given by

$$H_\rho = -\frac{\partial A_\phi}{\partial z} \tag{34}$$

$$H_\phi = -\frac{\partial A_\rho}{\partial z} \tag{35}$$

$$H_z = \frac{\partial A_\phi}{\partial \rho} + \frac{A_\phi}{\rho} - \frac{1}{\rho}\frac{\partial A_\rho}{\partial \rho} \tag{36}$$

The loop current across a section of the wire is found by integrating the function J_ϕ in Eq. (25) around the wire cross section. The loop radiation impedance is then the applied voltage V_0 in the gap divided by the current in the gap. Figure 7 shows the loop feed radiation resistance, and Fig. 8 shows the corresponding loop reactance, as a function of loop radius kr for a thin wire, $\Omega = 15$, and a thick wire, $\Omega = 10$, where $\Omega = 2\ln(2\pi b/a)$ is Storer's parameter (6). The thin-wire loop has very sharp resonant behavior compared with the thick-wire loop, especially for a half-wavelength diameter ($kb = 0.5$) structure. The higher resonances are less pronounced for both loops. Thick-wire loops exhibit an interesting behavior in that over a diameter of about a half wavelength, the reactance is

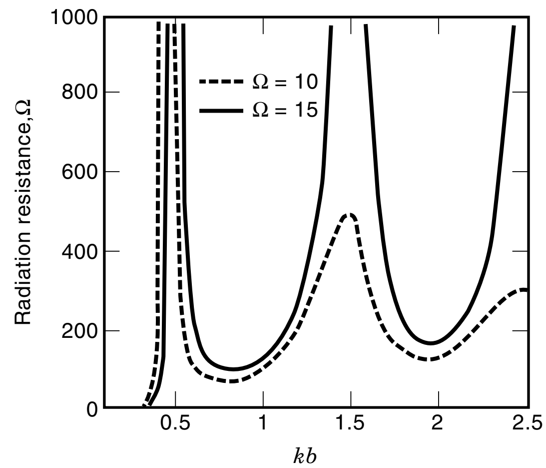

Figure 7. Loop radiation resistance.

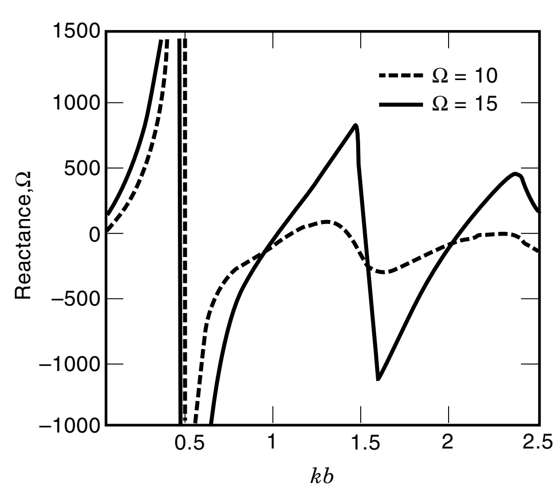

Figure 8. Loop reactance.

Table 1. Parameter Y for Various Loop Thicknesses and b = 0.01 Wavelengths

Ω	a/λ	Y
19.899	0.000003	−0.0039
17.491	0.00001	−0.0090
15.294	0.00003	−0.020
12.886	0.0001	−0.048
10.689	0.0003	−0.098
8.2809	0.001	−0.179

essentially always capacitive and the total impedance remains well behaved.

Small Gap-Fed Loops. The detailed analysis of the thick, gap-fed wire loop, as shown in Refs. 8 and 9, reveals that the current density around the circumference of the wire, angle ψ in Fig. 6, is not constant. An approximation to the current density along the wire circumference for a small diameter loop is

$$J_\phi = \frac{I_\phi}{2\pi a}[1 - 2\cos(\phi)(kb)^2][1 + Y\cos(\psi)] \tag{37}$$

where I_ϕ is the loop current, which has cosine variation along the *loop circumference,* and where the variation around the *wire circumference* is shown as a function of the angle ψ. Y is the ratio of the first- to the zero-order mode in ϕ and is not a simple function of loop dimensions a and b, but can be found numerically [Siwiak (2)] and from the analysis of the preceding section. For the small loop Y is negative and of order a/b so Eq. (37) predicts that there is current bunching along the inner contour (ψ = 180°) of the wire loop. Table 1 gives representative values for Y as a function of a/b.

This increased current density results in a corresponding increase in dissipative losses in the small loop. We can infer that the cross-sectional shape of the conductor formed into a loop antenna will impact the loss performance in a small loop.

The small loop fed with a voltage gap has a charge accumulation at the gap and will exhibit a close near electric field. For a small loop of radius b and in the x–y plane, the fields at $(x, y) = (0, 0)$ are derived in Ref. 9 and given here as

$$E_\phi = -j\,\frac{\eta_0 kI}{2} \tag{38}$$

where I is the loop current and

$$H_z = \frac{I}{2b} \tag{39}$$

Expression (39) is recognized as the classic expression for the static magnetic field within a single-turn solenoid. Note that the electric field given by Eq. (38) does not depend on any loop dimensions, but was derived for an electrically small loop. The wave impedance Z_w at the origin is the ratio of E_ϕ to H_z and from Eqs. (38) and (39) is

$$Z_w = -j\eta_0 kb \tag{40}$$

In addition to providing insight into the behavior of loop probes, Eqs. (38) to (40) are useful in testing the results of numerical codes, such as the numerical electromagnetic code (NEC) described in Ref. 3, and often used in the numerical analysis of wire antenna structures.

When the small loop is used as an untuned and unshielded field probe, the current induced in the loop will have a component due to the magnetic field normal to the loop plane as well as a component due to the electric field in the plane of the loop. A measure of E field to H field sensitivity is apparent from Eq. (40). The electric field to magnetic field sensitivity ratio of a simple small-loop probe is proportional to the loop diameter. The small gap-fed loop, then, has a dipole moment, which complicates its use as a purely magnetic field probe.

LOOP APPLICATIONS

Loop antennas appear in pager receivers as both ferrite-loaded loops and as single-turn rectangular shaped structures within the radio housing. When worn on a belt the loop benefits from coupling to the vertically resonant human body. In the high-frequency bands, the loop has been implemented as a series resonant circuit fed by a secondary loop. The structure can be tuned over a very large frequency band while maintaining a relatively-constant-feed point impedance. One-wavelength-perimeter square loops have been successfully implemented as high-gain transmitting structures.

The Ferrite-Loaded Loop Antenna—A Magnetic Dipole

Let us examine a small ferrite-loaded loop antenna with dimensions $2h$ = 2.4 cm, $2a$ = 0.4 cm, and at a wavelength of about λ = 8.6 m as pictured in Fig. 9. When the permeability of the ferrite is sufficiently high, this antenna behaves like a magnetic dipole. The magnetic fields are strongly confined to the magnetic medium, especially near the midsection of the ferrite rod, and behave as the dual of the electric dipole excited by a triangular current distribution. We can therefore analyze its behavior using a small dipole analysis shown by Siwiak (2). The dipole current is replaced by the equivalent magnetic current along the ferrite rod length $2h$.

The impedance at the midpoint of a short dipole having a current uniformly decreasing from the feed point across its length $2h$ is

$$Z_{\text{dipole}} = \frac{\eta_0}{6\pi}(kh)^2 - j\,\frac{\frac{\eta_0}{2\pi}\left[\ln\left(\frac{2h}{a}\right) - 1\right]}{kh} \tag{41}$$

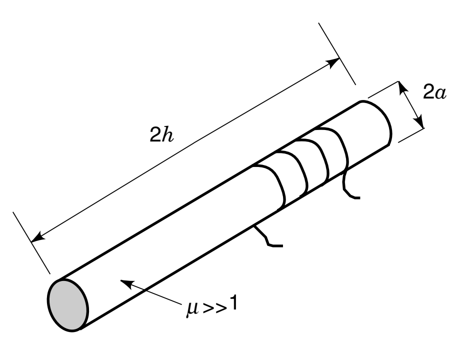

Figure 9. A ferrite-loaded loop antenna. [Source: Siwiak (2).]

The corresponding unloaded Q of the dipole antenna is

$$Q_{\text{dipole}} = \frac{3\left[\ln\left(\frac{2h}{a}\right) - 1\right]}{(kh)^3} \tag{42}$$

Equation (42) has the expected behavior of the inverse third power with size for small antennas, and for $h/a = 6$

$$Q_{\text{dipole}} = \frac{4.5}{(kh)^3} \tag{43}$$

Comparing the Q for a small dipole given by Eq. (43) with the Q of a small loop of Eq. (24) we see that the loop Q is small even though the same ratio of antenna dimension to wire radius was used. We conclude that the small loop utilizes the smallest sphere that encloses it more efficiently than does the small dipole. Indeed, the thin dipole, here masquerading as the analog of a long thin ferrite loaded loop, is essentially a one-dimensional structure, while the small loop is essentially a two-dimensional structure.

We can use Eqs. (41) and (42) for the elementary dipole to examine the ferrite-loaded loop antenna since it resembles a magnetic dipole. The minimum ideal Q of this antenna is given by Eq. (42), 1.01×10^6. The corresponding bandwidth of such an antenna having no dissipative losses would be 2×35 MHz $f/Q = 70$ MHz$/1.01 \times 10^6 = 69$ Hz. A practical ferrite antenna at this frequency has an actual unloaded Q_A of nearer to 100, as can be inferred from the performance of belt-mounted radios shown in Table 2. Hence, an estimate of the actual antenna efficiency is

$$10\log(Q_A/Q) = -40\,\text{dB} \tag{44}$$

and the actual resultant 3 dB bandwidth is about 700 kHz. Such an antenna is typical of the type that would be used in a body-mounted paging receiver application. As detailed by Siwiak (2), the body exhibits an average magnetic field enhancement of about 6 dB at this frequency, so the *average* belt-mounted antenna gain is −34 dBi. This is typical of a front position body-mounted paging or personal communication receiver performance in this frequency range.

Body Enhancement in Body-Worn Loop Antennas

Loops are often implemented as internal antennas in pager receiver applications spanning the frequency bands from 30 MHz to 960 MHz. Pagers are often worn at belt level and

Table 2. Paging Receiver Performance Using Loops

Frequency Band (MHz)	Paging Receiver, at Belt, Av. Gain (dBi)	Field Strength Sensitivity ($\text{dB}\cdot\mu\text{V/m}$)
30 to 50	−32 to −37	12 to 17
85	−26	13
160	−19 to −23	10 to 14
280 to 300	−16	10
460	−12	12
800 to 960	−9	18 to 28

Source: After Siwiak (2).

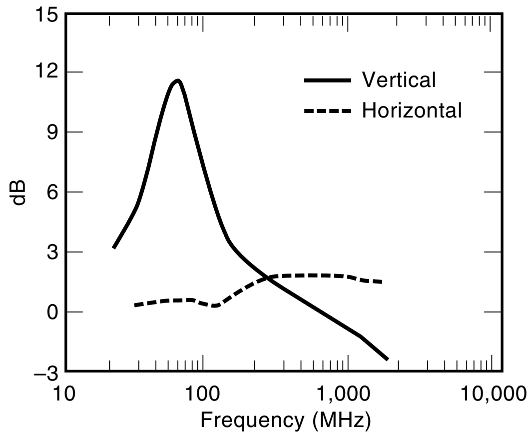

Figure 10. Gain-averaged body-enhanced loop response. [Source: Siwiak (2).]

benefit from the *body enhancement* effect. The standing adult human body resembles a lossy wire antenna that resonates in the range of 40 MHz to 80 MHz. The frequency response, as seen in Fig. 10, is broad, and for belt-mounted loop antennas polarized in the body axis direction, enhances the loop-antenna azimuth-averaged gain at frequencies below about 500 MHz.

The far-field radiation pattern of a body-worn receiver is nearly omnidirectional at very low frequency. As frequency is increased, the pattern behind the body develops a shadow that is manifest as a deepening null with increasing frequency. In the high-frequency limit, there is only a forward lobe with the back half-space essentially completely blocked by the body. For horizontal incident polarization there is no longitudinal body resonance and there is only slight enhancement above 100 MHz.

The Small Resonated High-Frequency Loop Antenna

The simple loop may be resonated with a series capacitor having a magnitude of reactance equal to the loop reactance, and indeed is effectively implemented that way for use in the high-frequency (HF) bands as discovered by Dunlavy (17). When fed by a second untuned loop, this antenna will exhibit a nearly constant-feed-point impedance over a 3 : 1 or 4 : 1 bandwidth by simply adjusting the capacitor to the desired resonant frequency. The reactive part of the loop impedance is inductive, where the inductance is given by $\text{Im}\{Z_L\} = \omega L$, so ignoring the higher-order terms

$$L = \frac{\eta_0 kb\left[\ln\left(\frac{8b}{a}\right) - 2\right]}{\omega} \tag{45}$$

which with the substitution $\epsilon_0 k/\omega = \mu_0$ becomes

$$L = \mu_0 b\left[\ln\left(\frac{8b}{a}\right) - 2\right] \tag{46}$$

The capacitance required to resonate this small loop at frequency f is

$$C = 1/(2\pi f)^2 L \tag{47}$$

The loop may be coupled to a radio circuit in many different ways, including methods given in Refs. 17 and 18. When used in transmitter applications, the small loop antenna is capable of impressing a substantial voltage across the resonating capacitor. For a power P delivered to a small loop with an unloaded Q of Eq. (23) and with resonating the reactance X_C given by the reactive part of Eq. (22), it is easy to show that the peak voltage across the resonating capacitor is

$$V_p = \sqrt{X_C QP} \tag{48}$$

by recognizing that

$$V_p = \sqrt{2} I_{rms} X_C \tag{49}$$

where I_{rms} is the total rms loop current

$$I_{rms} = \sqrt{\frac{P}{\mathrm{Re}\{Z_{loop}\}}} \tag{50}$$

along with Q at the resonant frequency in Eq. (23).

Transmitter power levels as low as 1 W delivered to a moderately efficient small-diameter (λ/100) loop can result in peak values of several hundred volts across the resonating capacitor. This is not intuitively expected: the small loop is often viewed as a high current circuit, which is often described as a short-circuited ring. However, because it is usually implemented as a *resonant circuit* with a resonating capacitor, it can also be an extremely-high-voltage circuit as will be shown later. Care must be exercised in selecting the voltage rating of the resonating capacitor even for modest transmitting power levels, just as care must be taken to keep resistive losses low in the loop structure.

As an example, consider the Q and bandwidth of a small loop antenna, $2b$ = 10 cm in diameter, resonated by a series capacitor and operating at 30 MHz. The example loop is constructed of $2a$ = 1 cm diameter copper rod with conductivity $\sigma = 5.7 \times 10^7$ S/m. The resistance per unit length of round wire of diameter $2a$ with conductivity σ is

$$R_s = \frac{1}{2\pi a \delta_s \sigma} = \frac{1}{2\pi a}\sqrt{\frac{\omega\mu_0}{2\sigma}} \tag{51}$$

where δ_s is the skin depth for good conductors, ω is the radian frequency, and $\mu_0 = 4\pi \times 10^{-7}$ H/m is the permeability of free space, so $R_s = 0.046\ \Omega$. From Eq. (22) the loop impedance is $Z = 0.00792 + 71.41j$. Hence the loop efficiency can be found by comparing the loop radiation resistance with loss resistance. The loop efficiency is $R_s/(R_s + \mathrm{Re}\{Z\}) = 0.147$ or 14.7%. From Eqs. (46) and (47) we find the resonating capacitance $C = 74.3\ \mu$F. From Eqs. (48) to (50) we see that if 1 W is supplied to the loop, the peak voltage across the resonating capacitor is 308 V and the loop current is 4.3 A. The *resonated* loop is by no means the "low-impedance" structure that we normally imagine it to be.

The Quad Loop Antenna

The quad loop antenna, sometimes called the cubical quad, was developed by Clarence C. Moore in the 1940s as a replacement for a four-element parasitic dipole array (Yagi–Uda array). The dipole array exhibited corona arcing at the element tips severe enough to damage the antenna when operated at high power levels (10 kW) in a high-altitude (10,000 ft) shortwave broadcasting application in the 25 m band. Moore sought an antenna design with "no tips" that would support extremely high electric field strengths that caused the destructive arcing. His solution was a one-wavelength-perimeter square loop, later with a loop director element as shown in Fig. 11. The configuration exhibited no arcing tendencies, and a new shortwave antenna configuration was born.

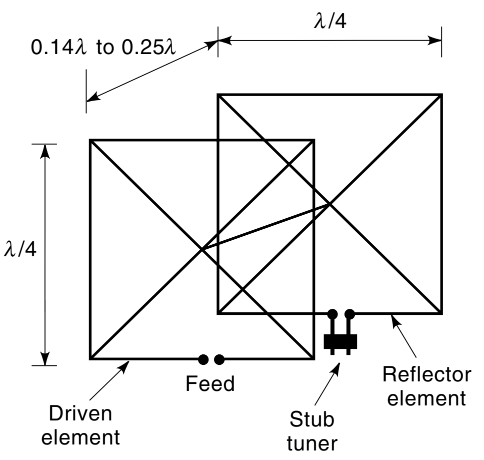

Figure 11. Two-element loop array.

As pictured in Fig. 11, the driven element is approximately one-quarter wavelength on an edge. Actually, resonance occurs when the antenna perimeter is about 3% greater than a wavelength. The reflector element perimeter is approximately 6% larger than a wavelength, and may be implemented with a stub tuning arrangement. Typical element spacing is between 0.14 and 0.25 wavelengths. The directivity of a quad loop is approximately 2 dB greater than that of Yagi antennas with the same element spacing.

BIBLIOGRAPHY

1. *IEEE Standard Definitions of Terms for Antennas,* IEEE Standard 145-1993, SH16279, 1993.
2. K. Siwiak, *Radiowave Propagation and Antennas for Personal Communications,* 2nd ed., Norwood, MA: Artech House, 1998.
3. G. J. Burke and A. J. Poggio, Numerical electromagnetics code (NEC)—method of moments, Lawrence Livermore Laboratory, *NOSC Tech. Document 116 (TD 116),* Vol. 1, 2, January 1981.
4. H. C. Pocklington, Electrical oscillations in wires, *Proc. Cambridge Phys. Soc. London,* **9**: 324–333, 1897.
5. E. Hallén, Theoretical investigation into transmitting and receiving qualities of antennae, *Nova Acta Regiae Soc. Ser. Upps.,* Vol. II, Nov. 4: 1–44, 1938.
6. J. E. Storer, Impedance of thin-wire loop antennas, *Trans. AIEE,* **75**: 609–619, 1965.
7. T. T. Wu, Theory of the thin circular antenna, *J. Math. Phys.,* **3**: 1301–1304, 1962.
8. Q. Balzano and K. Siwiak, The near field of annular antennas, *IEEE Trans. Veh. Technol.,* **VT36**: 173–183, 1987.
9. Q. Balzano and K. Siwiak, Radiation of annular antennas, *Correlations,* Motorola Engineering Bulletin, Schaumburg, IL: Motorola Inc., Vol. VI, No. 2, Winter 1987.

10. C. A. Balanis, *Advanced Engineering Elecromagnetics,* New York: Wiley, 1989.
11. R. E. Collin, *Antennas and Radiowave Propagation,* New York: McGraw-Hill, 1985.
12. E. C. Jordan and K. G. Balmain, *Electromagnetic Waves and Radiating Systems,* 2nd ed., Englewood Cliffs, NJ: Prentice-Hall, 1968.
13. R. Cohen and B. N. Taylor, The 1986 CODATA recommended values of the fundamental physical constants, *J. Res. Nat. Bur. Stand.,* **92** (2), 1987.
14. L. A. Hazeltine, Means for eliminating magnetic coupling between coils, US Patent No. 1,577,421, 1926.
15. R. W. P. King and C. W. Harrison, Jr., *Antennas and Waves: A Modern Approach,* Cambridge, MA: MIT Press, 1969.
16. R. Courant and D. Hibert, *Methods of Mathematical Physics,* New York: Interscience Publishers, 1953.
17. J. H. Dunlavy, Jr., Wide range tunable transmitting loop, US Patent No. 3,588,905, 28 June 1971.
18. T. Hart, Small, high-efficiency loop antennas, *QST,* **70** (6): 33–36, 1986.

KAZIMIERZ SIWIAK
Motorola, Inc.

LOOP PARALLELISM. See PROGRAM CONTROL STRUCTURES.

LORAN NAVIGATION. See RADIO NAVIGATION.